JAERI－Conf 2003－001

1.4.2 MODELING OF POSITRON STATES AND ANNIHILATION IN SOLIDS

M. J. Puska
Laboratory of Physics, Helsinki University of Technology
P.O. Box 1100, 02015 HUT, Finland

Abstract

Theoretical models and computational aspects to describe positron states and to predict positron annihilation characteristics in solids are discussed. The comparison of the calculated positron lifetimes, core annihilation lineshapes, and two-dimensional angular correlation maps with experimental results are used in identifying the structure (including the chemical composition) of vacancy-type defects and their development e.g. during thermal annealing. The basis of the modeling is the two-component density-functional theory. The ensuing approximations and the state-of-the-art electronic-structure computation methods enable practical schemes with a quantitative predicting power.

Keywords: Positron annihilation, density-functional theory, defects in solids

1 Introduction

Positron annihilation can be used as a versatile tool to investigate materials properties[1, 2, 3, 4, 5]. The applications extend from the advanced problems of solid state physics, such as the determination of the Fermi surfaces of metals or high-temperature superconductors, to the industrial materials testing during processes like damage development under irradiation or wear conditions. In between there are important materials physics studies like those for the electronic and ionic structures of vacancy-type defects in metals and in semiconductors. The last types of applications are in the focus of the present review. Especially, we will describe theoretical models and computational tools to calculate positron states and annihilation in solids. Theoretical predictions support in an essential way positron experiments for identifying defects in solids and for determining even their chemical structure.

The use of positron annihilation in defect studies is based on the trapping of positrons from a delocalized bulk state to a localized state at the defect. The trapping is due to the reduced nuclear repulsion at the open-volume defects. Because the electronic structure seen by the positron at the defect differs from that in the perfect bulk crystal the annihilation characteristics change. The positron lifetime increases because the average electron density decreases. For the same reason the momentum distribution of annihilating electron-positron pairs becomes more peaked at low momenta. However, the positron density may sample the different atomic species of a compound materials with different relative probabilities in the bulk and at a defect. The defect may be surrounded by impurity atoms. In these cases the high-momentum region of the distribution, which is mainly due to annihilations with core electrons, reflects the chemical structure of the defect. The changes in the bond structure between the atoms neighboring the defect may also affect the low-momentum part of the distribution. In order to understand these changes and fully benefit from them in defect identification, theoretical calculations with high predictive power are indispensable.

The purpose of this paper is to review the theory and computational methods used for describing positron states and annihilation in solids. The ideas are discussed by the help of selected applications. The rest of the paper is organized as follows. In Sec. 2, we first review the two-component density–functional theory on which the calculations for positrons in solids are based on. Thereafter, we introduce the so-called conventional scheme, which simplifies considerably the treatment of localized positron states. Finally, in Sec. 2 a fast method to predict positron states and annihilation, the atomic superposition method, is described. In Sec. 3 we discuss how the theory is tested by comparing the predictions with experiments and as an example of defect identification a study for As-vacancy complexes in silicon is reviewed. Finally, in Sec. 4 we provide conclusions and speculations on the future directions.

2 Theory and calculation methods

2.1 Electron and positron densities: The two–component density–functional theory

In the density–functional theory (DFT) [6] the total energy of an electron system is given as a functional of the electron density n_-. The ground–state electron density is calculated by minimizing this functional and thereafter, in principle, all the ground–state properties can be determined. In the two–component density–functional theory (TC-DFT) [7] for electron-positron systems in an external electrostatic potential $V_{ext}(\mathbf{r})$ the total energy is written as a functional of the electron and positron densities n_- and n_+ (in atomic units)

$$E[n_-, n_+] = \tag{1}$$
$$F[n_-] + F[n_+] - \int d\mathbf{r} V_{ext}(\mathbf{r})[n_-(\mathbf{r}) - n_+(\mathbf{r})] - \int d\mathbf{r} \int d\mathbf{r}' \frac{n_-(\mathbf{r})n_+(\mathbf{r}')}{|\mathbf{r} - \mathbf{r}'|} + E_c^{e-p}[n_-, n_+].$$

Above, $E_c^{e-p}[n_-, n_+]$ is the electron–positron correlation energy functional and the functional $F[n]$ reads as

$$F[n] = T[n] + \frac{1}{2} \int d\mathbf{r} \int d\mathbf{r}' \frac{n(\mathbf{r})n(\mathbf{r}')}{|\mathbf{r} - \mathbf{r}'|} + E_{xc}[n], \tag{2}$$

where $T[n]$ is the kinetic energy of noninteracting electrons or positrons. $E_{xc}[n]$ is the exchange–correlation energy between indistinguishable particles and $E_c^{e-p}[n_-, n_+]$ is the electron–positron correlation energy functional. The most commonly used approximation for $E_{xc}[n]$ is the local density approximation (LDA) where the exchange–correlation energy is approximated as

$$E_{xc}[n] = \int n(\mathbf{r}) \epsilon_{xc}(n(\mathbf{r})) d\mathbf{r}. \tag{3}$$

Above, $\epsilon_{xc}(n(\mathbf{r}))$ is the exchange–correlation energy per particle in a *homogenous* one-component electron gas. $\epsilon_{xc}(n(\mathbf{r}))$ can be determined accurately by the Quantum Monte-Carlo (QMC) method [8] and practical parametrizations exists for it [9]. In contrast, the electron–positron correlation energy has not yet been determined accurately by the QMC method due to statistics requirements to decribe the pile-up of the electron (positron) density at the positron (electron) [10]. For the electron–positron correlation energy at the limit of vanishing positron density Arponen and Pajanne [11] have provided results

on the basis of many-body perturbation expansions. At finite positron densities, the correlation energy functional was first calculated by Lantto [12] using the hypernetted chain approximation. Parametrizations are presented *e.g.* in Ref. [13]. The electron–positron correlation is usually also treated within the LDA.

From the above total energy functional, one derives the two-component Kohn-Sham equations for the electrons and positrons, *i.e.*

$$-\frac{1}{2}\nabla_i^2\psi_i(\mathbf{r}) + \left[\frac{\delta E_{xc}[n_-]}{\delta n_-(\mathbf{r})} - \phi(\mathbf{r}) + \frac{\delta E_c^{e-p}[n_-, n_+]}{\delta n_-(\mathbf{r})}\right]\psi_i(\mathbf{r}) = \epsilon_i\psi_i(\mathbf{r}), \tag{4}$$

$$-\frac{1}{2}\nabla_i^2\psi_i^+(\mathbf{r}) + \left[\frac{\delta E_{xc}[n_+]}{\delta n_+(\mathbf{r})} + \phi(\mathbf{r}) + \frac{\delta E_c^{e-p}[n_-, n_+]}{\delta n_+(\mathbf{r})}\right]\psi_i^+(\mathbf{r}) = \epsilon_i^+\psi_i^+(\mathbf{r}), \tag{5}$$

where

$$\phi(\mathbf{r}) = \int d\mathbf{r}' \frac{-n_-(\mathbf{r}') + n_+(\mathbf{r}') + n_0(\mathbf{r}')}{|\mathbf{r} - \mathbf{r}'|} \tag{6}$$

is the total Coulomb potential. Here, $n_0(\mathbf{r})$ denotes the positive ionic or nuclear charge density providing the external potential $V_{ext}(\mathbf{r})$. Because in the positron spectroscopy measurements there is only one positron in the solid sample at the time, one makes a self-interaction correction when calculating positron states [7, 13] by dropping out the self-Coulomb and self-exchange terms from Eq. (5).

The electron and positron densities are obtained by

$$n_-(\mathbf{r}) = \sum_{\epsilon_i \le \epsilon_F} |\psi_i(\mathbf{r})|^2; \qquad n_+(\mathbf{r}) = |\psi^+(\mathbf{r})|^2, \tag{7}$$

where ϵ_F is the electron Fermi energy. $\psi_i(\mathbf{r})$ and $\psi^+(\mathbf{r})$ are the Kohn–Sham single particle eigenstates for electrons and the positron, respectively.

Using the TC-DFT one can compute the Hellman–Feynman forces, caused by the electrons and positrons, acting on the *ions* and move the ions accordingly. It has been shown [14, 13, 15] that the positron induced relaxations around, say, vacancies in semiconductors can be considerably large and affect also the annihilation characteristics.

Solving Eqs. (4)-(7) self-consistently yields the electron and positron densities and allows one to calculate the positron annihilation characteristics, which can be directly compared with experiment. The positron annihilation rate is calculated within the LDA as

$$\lambda = \pi r_0^2 c \int d\mathbf{r} n_+(\mathbf{r}) n_-(\mathbf{r}) g(0; n_+(\mathbf{r}), n_-(\mathbf{r})), \tag{8}$$

where $g(0; n_+, n_-)$ is the electron–positron pair correlation function or the enhancement factor evaluated at the positron in a homogenous two–component plasma with positron density n_+ and electron density n_-. r_0 is the classical electron radius and c is the speed of light. The inverse of the annihilation rate is the positron lifetime.

The momentum distribution of the annihilating electron–positron pairs can be written as

$$\rho(\mathbf{p}) = \pi r_0^2 c \sum_i \left| \int d\mathbf{r} e^{-i\mathbf{p}\cdot\mathbf{r}} \psi_i^{ep}(\mathbf{r}, \mathbf{r}) \right|^2, \tag{9}$$

where $\mathbf{p}$ is the total momentum of the annihilating pair, $\psi_i^{ep}(\mathbf{r}, \mathbf{r})$ is the two–particle wave function when the positron and electron reside at the same point. The two–particle wave function is in principle difficult to calculate and therefore it is usually written in terms

of the positron and electron single–particle wave functions $\psi_+(\mathbf{r})$ and $\psi_i(\mathbf{r})$, respectively. Within the LDA one obtains

$$\psi_i^{\mathrm{ep}}(\mathbf{r},\mathbf{r}) = \psi_+(\mathbf{r})\psi_i(\mathbf{r})\sqrt{g(0;n_+(\mathbf{r}),n_-(\mathbf{r}))}, \tag{10}$$

where all the many–body effects have been buried into the enhancement factor $g(0;n_+,n_-)$.

2.2 Delocalized positron states and the conventional scheme

For a positron delocalized in a bulk solid, the density n_+ vanishes at every point and the above TC-DFT equations can be simplified considerably. Namely, the positron cannot affect the electronic structure which can be solved self–consistently by setting the correlation potential $\frac{\delta E_c^{e-p}[n_-,0]}{\delta n_-(\mathbf{r})}$ and the positron density to zero. Using the calculated electron density, one can then solve for the positron state from the Schrödinger equation with the potential

$$V_+(\mathbf{r}) = \phi(\mathbf{r}) + V_{corr}(n_-(\mathbf{r})), \tag{11}$$

where $\phi(\mathbf{r})$ is the Coulomb potential, obtained from the electronic structure calculation and V_{corr} is the zero–positron–density limit of the correlation potential $\frac{\delta E_c^{e-p}[n,n_+]}{\delta n_+(\mathbf{r})}$. Within the LDA, a commonly used form for this potential is the parametrization by Boroński and Nieminen [7] who used the data by Arponen and Pajanne [11]. It is possible to go beyond the LDA using the the generalized gradient approximation (GGA) [16] or the weighted density approximation (WDA) [17, 18] which take the inhomogenous caharacter of the electron density explicitly into account.

The calculation of the positron annihilation rate in Eq. (8) becomes also simpler for the delocalized positrons because the enhancement factor $g(0;0,n_-)$ depends only on the electron density. Instead of the LDA one can use for the enhancement factor the GGA [16] or the WDA [17, 18].

When calculating momentum distributions of annihilating electron-positron pairs Alatalo *et al.* [19] noticed that the LDA form of Eq. (10) may yield spurious effects at the high momentum region. They ended up using state-dependent enhancement factors and two-particle wavefunctions of the form

$$\psi_i^{\mathrm{ep}}(\mathbf{r},\mathbf{r}) = \psi_+(\mathbf{r})\psi_i(\mathbf{r})\sqrt{\lambda_j/\lambda_j^{\mathrm{IPM}}}, \tag{12}$$

where $\lambda_j^{\mathrm{IPM}} = \pi r_e^2 c \int d\mathbf{r}\psi_+^2(\mathbf{r})\psi_j^2(\mathbf{r})$ is the annihilation rate of the electron state ψ_j calculated using the independent-particle model (IPM) and λ_j is the annihilation rate obtained by a calculation utilizing the LDA or the GGA.

For a positron localized at a defect, the (average) density n_+ does not vanish and the above approximation is in principle invalid. Nevertheless, it has been widely applied since the calculations performed using the full two–component formalism tend to be time consuming and because the electron-positron correlation in the two-component plasma is inaccurately known. The ensuing scheme is called as the 'conventional' scheme. In the conventional scheme the electron density is first solved without the effect of the positron and then the positron state is calculated without any self-consistency iterations. The use of the conventional scheme can be justified by noticing that the positron and the electron screening cloud around it form a neutral quasiparticle which does not affect the average electron density of the system. Moreover, the results of the conventional scheme have been shown to be in agreement with those obtained by the two-component density-functional calculations [7, 13, 20].

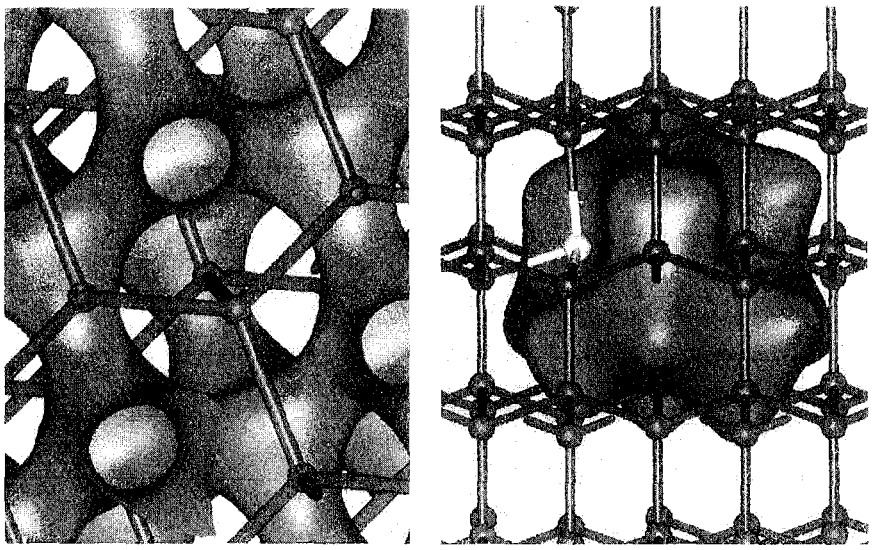

(a) (b)

Figure 1: (a) An isosurface of the positron wave function in a perfect Si lattice. The positions of the Si atoms are denoted by blue spheres, and the electronic interatomic bonds as blue sticks. The positron lifetime in this state is according to experiments and theory about 220 ps. (b) An isosurface of the positron wave function at a vacancy surrounded by one Sb impurity. The Sb atom is denoted by a yellow sphere. The positron lifetime in this state is according to theory about 230 ps [From Ref. [24]].

2.3 Numerical methods for positron calculations

Schemes and programs for the pure electron-structure calculations can be used also in the positron calculations. The potential felt by the positron can be constructed from the calculated electron density. The positron wavefunction can be presented using expansions similar to those for the electron states, and the momentum distributions can be calculated accordingly.

However, within the conventional scheme the practical calculations can be further simplified by using instead of a self-consistent electron density the superposition of (neutral) free atoms. The scheme obtained, called as the atomic superposition method[21], is fast and thereby especially beneficial for extended low-symmetry systems such as grain boundaries in solids or reconstructed surfaces (with adsorbates). Due to a compensation effect, *i.e.* the positron density follows the relaxation of the electron density keeping electron-positron overlap approximately unchanged, the positron lifetime is well estimated although the electron density is non-self-consistent. Of course, the momentum distribution of annihilating electron-positron pairs at low momenta is strongly affected by the bonding structure of valence electrons and it cannot be realiably calculated from atomic orbitals. But the high-momentum region is mainly due to the inert core electrons, and there the free atom wavefunctions can be used in the momentum calculation [19].

In the atomic superposition method the full three-dimensional positron potential is constructed in a three-dimensional point grid. The positron wavefunction can then be calculated in the same grid using a real-space Schrödinger equation solver. An especially efficient method is the Raleigh quotient multigrid (RQMG) method [22]. Because in the

multigrid scheme errors on all different lenghs scales are efficiently reduced, the method suits well for large systems. Indeed, with the RQMG method the solution of the positron wavefunction in a system of thousands of atoms is a matter of a few cpu-minutes on a normal workstation [23]. As an example of the use of the atomic superposition method, Fig. 1 shows the density of a positron delocalized in a perfect Si-lattice as well as that for a positron trapped by a vacancy defect in Si.

3 Examples of positron calculations

The theoretical models and computational schemes for positron states and annihilation characteristics can be first tested by comparing the predictions with well-characterized experimental results, usually with those for perfect bulk crystals. Thereafter the methods can be used in applications with experimental data, for example, in the defect identification. We follow this idea in the discussion of the present section.

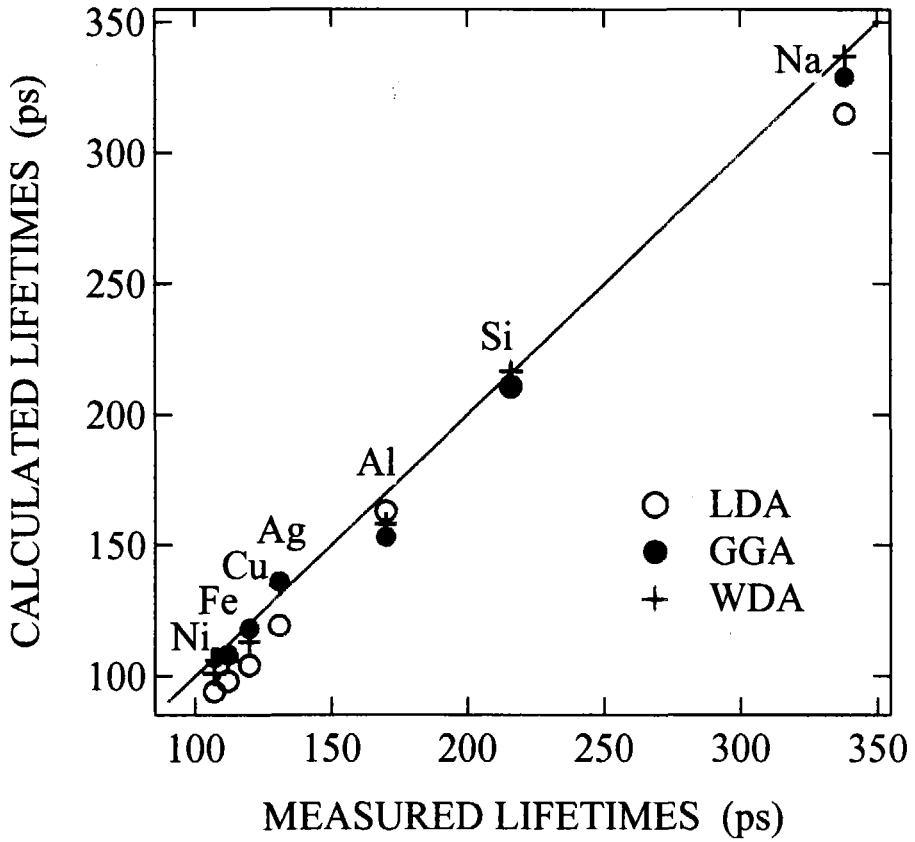

Figure 2: Calculated positron lifetimes in perfect bulk lattices as a function of the measured ones (The experimental values are quoted in Ref. [16]]). The open and solid circles give the LDA and the GGA results, respectively [16] whereas the crosses are obtained by the WDA [18].

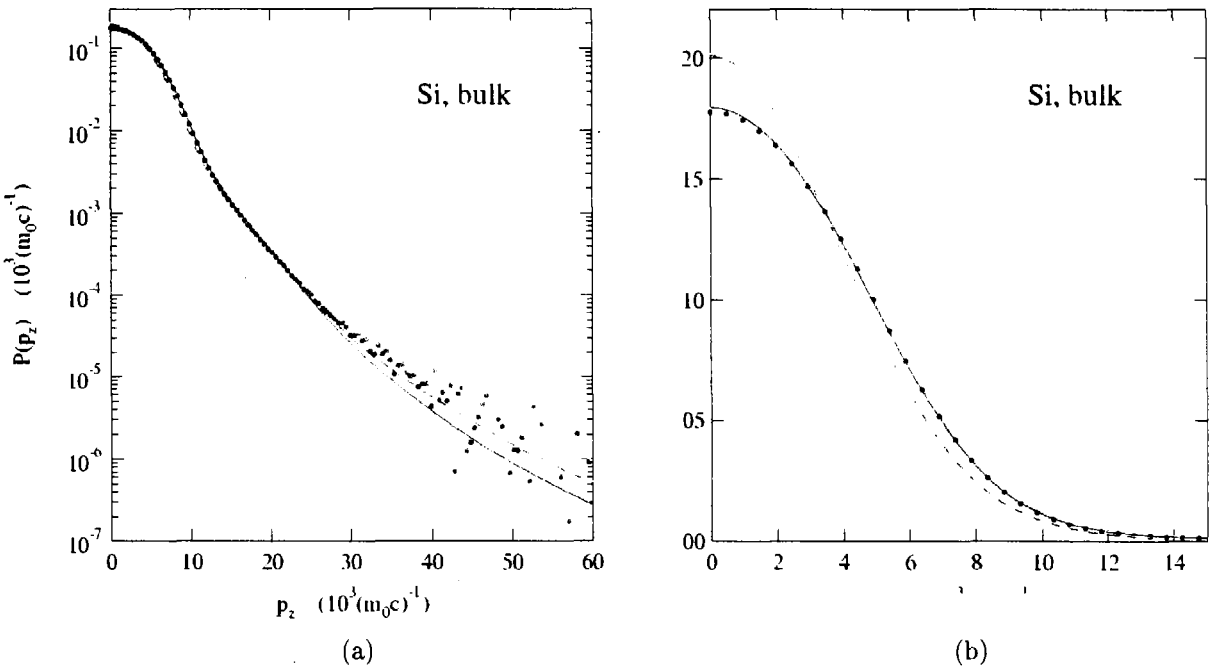

Figure 3: Positron annihilation probability density $P(p_z)$ for bulk Si. The experimental data (circles) [[36]] are shown together with two different theoretical calculations: (*i*) Self-consistent pseudo-valence-electron-density and free atom core (solid line) [[27]] (*ii*) Free atom valence and core electrons (dashed line). The theoretical curves are convoluted with a Gaussian in order to mimick the finite experimental resolution.

3.1 Comparisons between theoretical and experimental results

Positron lifetimes obtained by three different models for a selected set of bulk materials are compared in Fig. 2 with experimental data. The LDA calculation [4] uses the parametrization by Boroński and Nieminen [7] for the enhancement factor. In the GGA calculation [16] the enhancement factor is parametrized on the basis of the data by Arponen and Pajanne [11], whereas in the WDA calculation [18] the parametrization by Rubaszek and Stachowiak [25] is used in a state-dependent form. The LDA and WDA calculations do not use any adjustable parameters whereas there is one parameter in the GGA fitted to give an overall good agreement with experiment for a large number of bulk materials. All the works use in the numerical calculations of the self-consistent electronic structure and the positron state the linear-muffin-tin-orbital (LMTO) method. The overall agreement in comparison with experiment is good, especially in the case of the GGA and WDA. The GGA and the WDA have a tendency to decrease the positron annihilation with core electrons and thereby improve the agreement. The use of the non-self-consistent electronic structure and the atomic superposition method hardly affects the results on the LDA level and the changes are usually small within the GGA, too [16]. In conclusions, for the positron lifetimes the choice of the scheme is not very important in practice. More

important is that in defect identification one compares the differences between the bulk and defect lifetimes, so that possible systematic errors cancel.

The calculated momentum distributions of the annihilating electron-positron pairs can be compared with spectra of the two-dimensional angular correlation of annihilation radiation (2D-ACAR) and the coincidence Doppler-broadening (CDB) methods [1]. The 2D-ACAR gives detailed information about the valence electron momentum distribution integrated over one spatial direction. It is also possible to construct three-dimensional momentum distributions from the 2D-ACAR data [26]. The CDB technique gives momentum distributions integrated over two perpendicular directions. The CDB technique has been recently reviewed by Alatalo and Puska [5].

Fig. 3 compares CDB spectra (or the positron annihilation probability densities) for bulk Si simulated by two theoretical schemes with the measured one. One of the calculations uses the self-consistent valence electron density obtained with the pseudo-potential-plane-wave method and free atom core densities [27]. The fully three-dimensional positron wavefunction is used with valence electrons whereas a spherically symmetric positron wavefunction is assumed when calculating the core electron contribution to the momentum density. In the other calculation [5] the fast scheme by Alatalo *et al.* [19] is employed. In this scheme the free atom orbitals are used for all electrons. Furheron, the annihilation rates λ_j are calculated by using the fully three-dimensional positron wavefunction but the integral in Eq. (9) is performed by assuming spherically symmetric functions. Both of the calculations use the GGA for the annihilation rates and the state-dependent enhancement scheme of Eq. (12). In order to describe the low-momentum region the self-consistent valence electron density is necessary. But for the high-momentum part the non-self-consistent electron density is sufficient.

The case of bulk Si in Fig. 3 is perhaps easy to model with the present theories. The most accurate all-electron calculations [28] have resulted in a good agreement with experiment also in the case of bulk Al and graphite. They show that the spherical approximation for the positron state is good for Al. But for graphite, having a layer structure, the full three-dimensional positron wavefunction should be used. In the case of materials having 3d valence or semicore orbitals the above mentioned state-dependent enhancement gives usually too high intensities at high momenta in comparison with experiment [19]. Momentum (or energy) -dependent enhancement schemes may improve the situation [29, 30]. However, the struggle toward improvements may be hindered by the fact that the results seem to be sensitive to the details of the electronic structure calculation [31].

3.2 Applications in defect identification

The comparison of computed and measured positron annihilation characteristics has been intensively used in defect identification for several decades. One of the first works was the size-determination of small voids or vacancy agglomerates in neutron-irradiated metals by comparing the measured and calculated positron lifetimes [32]. Thereafter, theoretical predictions have been benefitted especially in the identification of structures of vacancy-defects and vacancy-impurity complexes in elemental and compound semiconductors [3]. In semiconductors, there are many possible defects trapping positrons. Therefore the combination of several experimental methods, such as the positron lifetime and coincidence Doppler broadening spectroscopies, with the theoretical work is necessary. In this review, we will consider the identification of vacancy-impurity complexes in As-doped Si as an example.

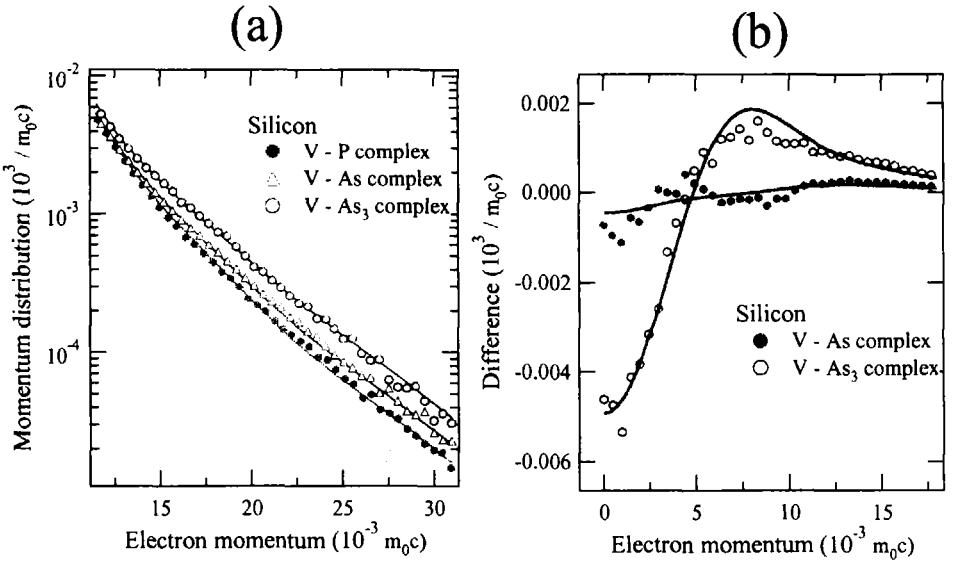

Figure 4: (a) High-momentum parts of the positron-electron momentum distributions. Measured results for positrons trapped in electron-irradiated P-doped (filled circles), electron-irradiated As-doped (triangles), and as-grown As-doped Si (open circles) samples as well as calculated distributions (solid lines) for vacancy-P, vacancy-As, and vacancy-As_3 complexes are shown. (b) Momentum differences of vacancy-As and vacancy-As_3 complexes with respect to the momentum distribution at the vacancy-P complex. The measured and calculated results are given by markers and solid lines, respectively [From Ref. [33]].

In a recent work, Saarinen *et al.* [33] used positron lifetime and CDB measurements in identifying structures of vacancy-impurity complexes in highly As-doped Si and discussed the As diffusion processes. The work shed thereby new light on the problem of the nature of compensating defects causing the saturation of the free electron densities at high doping levels. The measurements were complemented by calculations of the positron parameters. Valence electron structures were solved in the supercell approximation using the pseudopotential-plane-wave method. Free-atom core charge densities were superimposed in the pseudo-valence-electron density when calculating positron states and annihilation.

Measurements were performed for as-grown As-doped ([As] = 10^{20} cm$-$3) Si as well as for electron-irradiated P-doped ([P] = 10^{20} cm$-$3) and As-doped ([As] = 10^{20} cm$-$3) Si samples. According to the measurements, positrons are trapped in irradiated samples in irradiation-induced vacancy-type defects and annihilate with the lifetime of $\sim$250 ps which is clearly longer than that in perfect bulk, 220 ps. In the as-grown sample part of the positrons are trapped by vacancy-type defects and have also a lifetime of $\sim$250 ps. According to the theoretical calculations this lifetime corresponds to a single vacancy in Si and the lifetime is quite insensitive if neighboring Si atoms are substituted by impurities. There are, however, large differences in the positron-electron momentum distributions (Doppler spectra) for the trapped positrons as shown in Fig. 4. The measured distributions for electron-irradiated P-doped, electron-irradiated As-doped, and as-grown As-doped Si samples agree with the calculated distributions for positrons trapped at a single vacancy decorated with one P, one As, and three As atoms, respectively. The annihilation with As 3d-electrons raises the intensity at high momenta (Fig. 4a) rather

linearly as a function of the number of As atoms neighboring the vacancy. As shown in Fig. 4b, using the differences in momentum distributions, the agreement between theory and measurements is very good also at low momenta where the valence electron contributions dominate. Calculations assuming positron trapping at vacancies decorated with two or four neighboring As atoms do not result in agreement.

The main result of the work by Saarinen *et al.* is that complexes of a vacancy and three As atoms are formed in as-grown highly As-doped Si. These complexes are electronically inactive and account therefore for the observed saturation of the free electron density. The formation of the $V - As_3$ complexes is in agreement with the theoretical model for defect formation and diffusion by Ramamoorthy and Pantelides [34]. According to this model the formation energies for $V - As_n$, n > 2, are negative so that their formation is limited only by the diffusion of their constituent defects. At high temperatures the As diffusion starts by formation of $V - As$ -pairs. If As concentration is high enough there may be a second As-impurity as a fifth or closer neighbor of the first one and the migration of the As-V pair leads to the formation of the $V - As_2$ complex [35]. Ramamoorthy and Pantelides introduced a model according to which the diffusion of $V - As_2$ is very fast. The complex migrates through the lattice until it is captured by an other defect. With the highest probability this defect is a substitutional As impurity and a $V - As_3$ complex is formed. The scheme explains the abundance of the $V - As_3$ complexes and the missing of the $V - As_2$ complexes in samples of high As concentration. Recently, Ranki *et al.* [37] complemented the study by measuring the migration energies of the $V - As$ and $V - As_2$ pairs. They used electron irradiated As doped samples and performed thermal annealing.

4 Conclusion

Theoretical models and computational methods for positron states and annihilation characteristics in solids have reached the level of quantitative predicting power and an important status in the analysis of experimental data. Simple methods, such as the atomic superposition can give the first insight to the physical situation in question. The atomic superposition results are often even of high quantitative accuracy. This is especially true when predicting positron lifetimes and momentum densities of annihilating electron-positron pairs at high momenta. However, care has to taken in order to realize the limits of the method used. For example, the use of the self-consistent valence electron structure is necessary for the quantitative prediction of the momentum densities at low momenta. The self-consistent solution, including the determination of ion positions, may be necessary also when calculating positron states and lifetimes for defects in semiconductors. Finally, one should not forget the development of the theory of positron-electron interaction especially for a localized positron in an inhomogenous electron gas. Quantum Monte Carlo calculations would be indispensable for this purpose.

References

[1] R. Krause-Rehberg and H. S. Leipner, *Positron Annihilation in Semiconductors*, (Springer, Heidelberg, 1999).

[2] A. Dupasquier and A. P. Mills Jr. (Eds.) *Positron Spectroscopy of Solids*, (IOS Press, Amsterdam, 1995).

[3] K. Saarinen, P. Hautojärvi, and C. Corbel, in *Identification of Defects in Semiconductors*, edited by M. Stavola (Academic, New York, 1998).

[4] M. J. Puska and R. M. Nieminen, Rev. Mod. Phys, **66**, 841 (1994).

[5] M. Alatalo and M. J. Puska, Advances in Quantum Chemistry, in print.

[6] R. O. Jones and O. Gunnarsson, Rev. Mod. Phys. **61**, 689 (1989).

[7] E. Boroński and R. M. Nieminen, Phys. Rev. B **34**, 3280 (1986); R. M. Nieminen, E. Boroński, and L. J. Lantto, Phys. Rev. B **32**, 1377 (1985).

[8] D. M. Ceperley and B. J. Alder, Phys. Rev. Lett. **45**, 566 (1980).

[9] J. Perdew and A. Zunger, Phys. Rev. B **23**, 5048 (1981).

[10] L. Gilgien, *Modeling positron-electron correlations in condensed matter systems*, Thesis, University of Geneve, 1997.

[11] J. Arponen and E. Pajanne, Ann. Phys. (N.Y.) **121**, 343 (1979).

[12] L. J. Lantto, Phys. Rev. B **36**, 5160 (1987).

[13] M. J. Puska, A. P. Seitsonen, and R. M. Nieminen, Phys. Rev. B **52**, 10 947 (1995).

[14] L. Gilgien, G. Galli, F. Gygi, and R. Car, Phys. Rev. Lett. **72**, 3214 (1994).

[15] M. Saitoand A. Oshiyama, Phys. Rev. B **53**, 7810 (1996).

[16] B. Barbiellini, M.J. Puska, T. Torsti and R.M. Nieminen, Phys. Rev. B **51**, 7341 (1995); B. Barbiellini, M.J. Puska, T. Korhonen, A. Harju, T. Torsti and R.M. Nieminen, Phys. Rev. B **53**, 16 201 (1996).

[17] K. Jensen and A. B. Walker, J. Phys. F **18**, L277 (1988).

[18] A. Rubaszek, Z. Szotek, and W. Temmerman, Phys. Rev. B **58**, 11 285 (1998).

[19] M. Alatalo, B. Barbiellini, M. Hakala, H. Kauppinen, T. Korhonen, M. J. Puska, K. Saarinen, P. Hautojärvi, and R. M. Nieminen, Phys. Rev. B **54**, 2397 (1996).

[20] T. Korhonen, M. J. Puska, and R. M. Nieminen, *First-principles calculation of positron annihilation characteristics at metal vacancies*, Phys. Rev. B **54**, 15 016 (1996).

[21] M. J. Puska, and R. M. Nieminen, J. Phys. F **13**, 2695 (1983).

[22] J. Mandel and S. McCormick, J. Comput. Phys. **80**, 442 (1989); M. Heiskanen, T. Torsti, M.J. Puska, and R.M. Nieminen, Phys. Rev. B **63**, 245106 (2001).

[23] T. Torsti *et al.* unpublished.

[24] M. Hakala and M. J. Puska, unpublished.

[25] A. Rubaszek and H. Stachowiak, Phys. Status Solidi B **124**, 159 (1984).

[26] M. Saito, A. Oshiyama, and S. Tanigawa, Phys. Rev. B **44**, 10 601 (1991).

[27] M. Hakala, M. J. Puska, and R. M. Nieminen, Phys. Rev. B **57**, 7621 (1998).

[28] Z. Tang, M. Hasegawa, Y. Nagai, M. Saito, and Y. Kawazoe, Phys. Rev. B **65**, 045 108 (2002).

[29] A. Rubaszek, Z. Szotek, and W. M. Temmerman, Phys. Rev. B **61**, 10100 (2000).

[30] H. Sormann, G. Kontrym–Sznajd, and R. N. West, Mater. Sci. Forum **363–365**, 609 (2001).

[31] H. Sormann and M. Šob, Phys. Rev. B **64**, 045 102 (2001).

[32] P. Hautojärvi, J. Heiniö, M. Manninen, and R. M. Nieminen, Phil. Mag. **35**, 973 (1977).

[33] K. Saarinen, J. Nissilä H. Kauppinen, M. Hakala, M. J. Puska, P. Hautojärvi, and C. Corbel, Phys. Rev. Lett. **82**, 1883 (1999).

[34] M. Ramamoorthy and S. T. Pantelides, Phys. Rev. Lett. **76**, 4753 (1996).

[35] D. Mathiot and J. C. Pfister, Appl. Phys. Lett. 42 (1983) 1043.

[36] K. Saarinen and V. Ranki, unpublished.

[37] V. Ranki, J. Nissilä, and K. Saarinen, Phys. Rev. Lett. **88**, 105506 (2002).